# The LHCb experiment

on behalf of the LHCb Collaboration
Tatsuya Nakada[a]*

[a]CERN, CH-1211 Geneva 23, Switzerland
and
Institut de Physique des Hautes Energies, University of Lausanne
CH-1015 Dorigny, Switzerland

The LHCb experiment is designed to fully exploit the large number of b hadrons expected at the LHC energy and luminosity. The experiment is equipped with particle identification devices and can efficiently trigger events with different B-meson final states, allowing systematic studies of CP violation and other rare phenomena in the b hadron system with a high precision which could reveal physics beyond the Standard Model.

## 1. PHYSICS CASE

Well established CP violation phenomena in the neutral kaon system can be described in a consistent manner within the framework of the Standard Model[1]. However, no real precision test has been made due to the large uncertainties in evaluating the effect of hadronic interactions. The Standard Model can make very precise predictions for CP violation in some B-meson decay modes without hadronic uncertainties once all the four parameters of the Cabibbo-Kobayashi-Maskawa[2] (CKM) mass mixing matrix become known. Therefore, it is now widely accepted that the B-meson system provides an ideal place for testing the Standard Model for CP violation.

BaBar, Belle, CDF, D0 and HERA-B are the experiments which will soon establish CP violation in $\mathrm{B_d^0}$ and $\mathrm{\overline{B}_d^0}\rightarrow\mathrm{J}/\psi\mathrm{K_S}$ decays if CP violation is indeed largely due to the Standard Model. In the framework of the Standard Model, this will already allow to test the consistency of the determined CKM parameters. The situation becomes more complicated if physics beyond the Standard Model is present and CP violation measurements with other than the $\mathrm{J}/\psi\mathrm{K_S}$ final states become necessary as demonstrated in the following sections.

Interest in CP violation is not limited to elementary particle physics. It is one of the three necessary ingredients to generate observed excess of matter over antimatter in the universe[3]. The amount of CP violation which can be generated by the Standard Model appears to be insufficient for explaining the observed matter-antimatter asymmetry in the universe[4], giving a strong motivation to search for new physics.

*Permanent address: PSI, CH-5232 Villigen-PSI, Switzerland

### 1.1. The standard model scenario

Quark mixing in the Standard Model is described by the unitary CKM matrix $V$

$$V = \begin{pmatrix} V_{\mathrm{ud}} & V_{\mathrm{us}} & V_{\mathrm{ub}} \\ V_{\mathrm{cd}} & V_{\mathrm{cs}} & V_{\mathrm{cb}} \\ V_{\mathrm{td}} & V_{\mathrm{ts}} & V_{\mathrm{tb}} \end{pmatrix}$$

with four independent parameters. Using the Wolfenstein parameterization [5] with $\lambda$, $A$, $\rho$ and $\eta$, the matrix can be expanded in powers of $\lambda \approx 0.02$, the well determined sine of the Cabibbo angle, and CP violation is generated by a non-zero value of $\eta$. The relevant elements for the B-meson system are

$$V_{\mathrm{tb}} \approx 1,\ V_{\mathrm{cb}} \approx A\lambda^2,\ V_{\mathrm{ts}} \approx -A\lambda^2(1+i\lambda^2\eta),\ V_{\mathrm{ub}} \approx A\lambda^3(\rho - i\eta),\ V_{\mathrm{ts}} \approx A\lambda^3[1-\hat{\rho}-i\hat{\eta}]$$

where $\hat{\rho}, \hat{\eta} = (1-\lambda^2/2)\rho, \eta$.

From the B-meson decays with charm mesons in the final states, in particular the semileptonic decays, $|V_{\mathrm{cb}}|^2$ is determined and then used to extract $A$. Similarly, the semileptonic B-meson decays with no charm particle in the final state give $|V_{\mathrm{ub}}|^2$, i.e. $A^2\lambda^6[\rho^2+\eta^2]$. The measured frequency of $\mathrm{B_d^0}$-$\overline{\mathrm{B}}_\mathrm{d}^0$ oscillations gives the modulus of the $\mathrm{B_d^0}$-$\overline{\mathrm{B}}_\mathrm{d}^0$ oscillation amplitude. In the Standard Model, the $\mathrm{B_d^0}$-$\overline{\mathrm{B}}_\mathrm{d}^0$ oscillations are generated by the box diagrams with W's and up-type quarks in the loop. Among the various up-type quarks, only the top quark plays a role. Therefore, the modulus of the $\mathrm{B_d^0}$-$\overline{\mathrm{B}}_\mathrm{d}^0$ oscillation amplitude is proportional to $|V_{\mathrm{td}}|^2$, i.e. the $\mathrm{B_d^0}$-$\overline{\mathrm{B}}_\mathrm{d}^0$ oscillation frequency measures $A^2\lambda^6[(1-\hat{\rho})^2+\hat{\eta}^2]$. With all those measurements, $A$, $\rho$ and $\eta$ can be determined[2].

In the Wolfenstein parameterization, the phases of $V_{\mathrm{ub}}$, $V_{\mathrm{td}}$ and $V_{\mathrm{ts}}$ are given by $-\gamma$, $-\beta$ and $\delta\gamma + \pi$, respectively, which can be defined by $\rho$ and $\eta$ as

$$\gamma = \tan^{-1}\left(\frac{\eta}{\rho}\right), \quad \beta = \tan^{-1}\left(\frac{\hat{\eta}}{1-\hat{\rho}}\right), \quad \delta\gamma = \tan^{-1}\lambda^2\eta.$$

In the Standard Model, the phase of the $\mathrm{B_d^0}$-$\overline{\mathrm{B}}_\mathrm{d}^0$ oscillation amplitude is given by $2\arg V_{\mathrm{td}} = -2\beta$. As is well known, CP asymmetry between the time dependent rate of the initial $\mathrm{B_d^0}$ decaying into $\mathrm{J}/\psi\mathrm{K_S}$ and that of the initial $\overline{\mathrm{B}}_\mathrm{d}^0$ decaying into $\mathrm{J}/\psi\mathrm{K_S}$ measures the sum of the phase of $\mathrm{B_d^0}$-$\overline{\mathrm{B}}_\mathrm{d}^0$ oscillation amplitude and that of $\mathrm{B_d^0}\to\mathrm{J}/\psi\mathrm{K_S}$ decay amplitude. The $\mathrm{B_d^0}\to\mathrm{J}/\psi\mathrm{K_S}$ decay is largely due to the $\overline{\mathrm{b}} \to \overline{\mathrm{c}} + \mathrm{W}^+$ tree diagram, thus the decay amplitude is real. There exist a small contribution from the penguin diagrams. However, the decay amplitude of the most dominant penguin diagram with the top quark in the loop is proportional to $V_{\mathrm{tb}}^* V_{\mathrm{ts}}$ and has only a very small phase $\delta\gamma$. Therefore, the phase of the $\mathrm{B_d^0}\to\mathrm{J}/\psi\mathrm{K_S}$ decay amplitude is 0 to a very good approximation. In conclusion, the CP asymmetry in $\mathrm{B_d^0}\to\mathrm{J}/\psi\mathrm{K_S}$ and $\overline{\mathrm{B}}_\mathrm{d}^0\to\mathrm{J}/\psi\mathrm{K_S}$ measures the phase of $\mathrm{B_d^0}$-$\overline{\mathrm{B}}_\mathrm{d}^0$ oscillation amplitude, i.e. $-2\beta$. By comparing the $\beta$ with the value determined by $\rho$ and $\eta$ obtained from $|V_{\mathrm{td}}|$ and $|V_{\mathrm{ub}}|$ measurements, consistency of the Standard Model can be tested. This test will be well performed by the current generation of the experiment.

---

[2]There are two solutions corresponding to $\pm\eta$. Among the two, $\eta > 0$ is selected if the observed CP violation in the $\mathrm{K}^0$-$\overline{\mathrm{K}}^0$ has to be explained within the Standard Model.

### 1.2. Scenario with new physics

In the semileptonic decays, new physics has to compete with the Standard Model contribution in the tree process, $b \rightarrow c + W$ followed by $W \rightarrow \ell + \nu$. Here, new physics is expected contribute very little to the processes. Therefore the semileptonic B-meson decays extract $|V_{cb}|^2$ and $|V_{ub}|^2$; i.e. $A$ and $\rho^2 + \eta^2$ can be obtained even physics beyond the Standard Model is present.

New physics could generate $B_d^0$-$\overline{B}_d^0$ and $B_s^0$-$\overline{B}_s^0$ oscillations with new particles contributing to the box diagrams. New particles could also generate the oscillations through the tree diagrams. Since the Standard Model contribution to the oscillations is in the second order, the effect from the new physics may not be negligible. Both the modulus and phase of the $B_d^0$-$\overline{B}_d^0$ and $B_s^0$-$\overline{B}_s^0$ oscillation amplitudes would be modified, and the oscillation frequency of the $B_d$-meson system would yield $A^2\lambda^6[(1-\hat{\rho})^2 + \hat{\eta}^2] + r_{bd}$ where $r_{bd}$ is the contribution from new physics. Similarly, the oscillation frequency of the $B_s$-meson system would yield $A^2\lambda^4 + r_{bs}$ where $r_{bs}$ is the contribution from new physics.

Unlike in the case of the Standard Model scenario, $\eta$ and $\rho$ can no longer be determined only with those measurements.

Now we consider CP violation. The decay process $B_d^0$ into $J/\psi K_S$ is totally dominated by the tree diagram $\overline{b} \rightarrow \overline{c} + W^+$ and any contribution from new physics can be neglected in the decay amplitude. Therefore, CP asymmetry between the time dependent rate of the initial $B_d^0$ and that of the initial $\overline{B}_d^0$ decaying into $J/\psi K_S$ measures $-2\beta + \phi_{bd}$, where $\phi_{bd}$ is the phase of new physics contributing to the $B_d^0$-$\overline{B}_d^0$ oscillation amplitude.

CP violation measurement done with the time dependent rates for the initial $B_d^0$ decaying into $D^{*+}\pi^-$ and $D^{*-}\pi^+$and those for the CP conjugated processes involves three phases: the phase of $B_d^0$-$\overline{B}_d^0$ oscillation amplitude, that of the $B_d^0 \rightarrow D^{*+}\pi^-$ decay amplitude and that of the $B_d^0 \rightarrow D^{*-}\pi^+$ decay amplitude. No contribution from new physics is expected in $B_d^0$ decay amplitudes into $D^{*+}\pi^-$ and $D^{*-}\pi^+$. Therefore, CP violation in $B_d^0 \rightarrow D^{*+}\pi^-$, $B_d^0 \rightarrow D^{*-}\pi^+$ and the CP conjugated decays of the two gives $-2\beta + \phi_{bd} - \gamma$. By combining the two measurements, we obtain $\gamma$.

With this measured $\gamma = \tan^{-1}\eta/\rho$ combined with $\rho^2 + \eta^2$, we can now obtain $\eta$ and $\rho$, hence all the Wolfenstein's parameters are determined. The parameters for new physics, $r_{bd}$ and $\phi_{bd}$, can also be extracted. From the $B_s^0$ sector, $\gamma$ can be determined by combining CP violation in $J/\psi\phi$ decay modes and $D_sK$ decay modes, providing a nice consistency test together with the parameters for the new physics contribution, $r_{bs}$ and $\phi_{bs}$.

CP violation measurements with these decay modes by the current generation of the experiments will be rather poor if not impossible due to the limited event statistics and/or detector capabilities. This calls for a new dedicated experiment placed at intensive source of B mesons. LHC will be the most intense source of b-mesons providing not only $B_u$ and $B_d$, but also $B_s$ and $B_c$. The experiment should be able to trigger both the final states containing leptons and those with only hadrons. Particle identification, in particular the $K/\pi$ separation, is essential for reconstructing hadronic final states. In order to observe CP violation in the rapidly oscillating $B_s$-meson system, an excellent decay time resolution is required. The LHCb spectrometer is designed to fulfill these requirements.

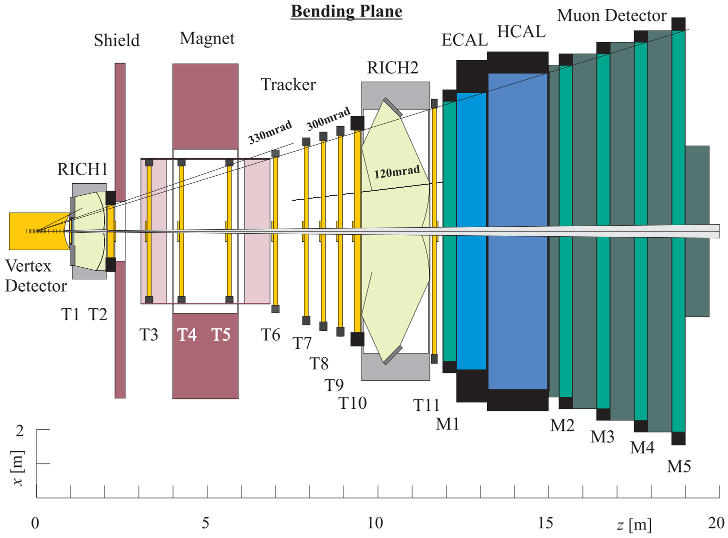


Figure 1. The LHCb spectrometer.

## 2. LHCb SPECTROMETER

Figure 1 illustrates the LHCb spectrometer [6]. It resembles a typical fixed target spectrometer, consists of a vertex detector at the intersection point (placed in "Roman pots"), a tracking system, RICH counters with aerogel and gas radiators, a large-gap dipole magnet, a calorimeter system, and a muon system.

The choice of the detector geometry is based on the fact that both the b- and $\overline{\mathrm{b}}$-hadrons are predominantly produced in the same forward cone at high energies. This feature is essential for the flavour tag.

IP-8, the experimental area currently occupied by the DELPHI experiment, will be used for the LHCb experiment. At IP-8, the pp collision point will be displaced by $\sim 11$ m so that large detector components such as the magnet, calorimeters and muon system can be placed in the already existing hall. Therefore, no extra excavation is required.

### 2.1. Magnet

The spectrometer dipole magnet is placed right after RICH-1. A normal conducting magnet provides a field integral of 4 Tm. The polarity of the field can be changed to reduce systematic errors in the CP-violation measurements that could result from a left-right asymmetry of the detector. An iron shield upstream of the magnet reduces the stray field in the vicinity of the vertex detector and of RICH-1.

### 2.2. Vertex detector

A total of 19 layers of silicon microstrip detectors are placed perpendicular to the beam, of which 17 layers are used as a vertex detector system. The remaining two layers are dedicated for detecting bunch crossings with more than one pp interactions as a part of the Level-0 trigger (pile-up veto counter). Each layer of the vertex detector system consists of two planes with $r$ and $\phi$ strips respectively. The $r$-strips provide azimuthal and the

$\phi$-strips radial coordinates. Pile-up veto counters consist of $\phi$-strip planes only. These strip configurations are chosen to make an efficient trigger algorithm. The closest distance between the active silicon area and the beam is 1 cm. The silicon detectors are placed in Roman pots with 100 mm thick aluminum windows, which act as a shield against RF pickup of the circulating beams. In order to avoid collapse of the windows, a secondary vacuum is maintained inside the Roman pots. During the injection and acceleration, the Roman pot system will be moved away from the beam to avoid interference with the machine operation and accidental irradiation of the detectors.

### 2.3. Tracking system

Because of the high particle density close to the beam pipe, the LHCb tracking detector is split into inner and outer systems. The inner tracking chambers have dimensions of $60 \times 40$ cm$^2$. Drift chambers based on Straw technology are considered as baseline for the outer tracking detector. For the inner tracking system where high granularity is required, various options including Micro Cathode Strip Chambers (MCSC's) with Gaseous Electron Multipliers (GEM's) are being considered.

### 2.4. RICH detectors

The RICH system of the LHCb detector consists of two detectors with three different radiators in order to cover the required momentum range, 1-150 GeV/$c$. The first detector uses aerogel and $C_4F_{10}$ gas as radiators. The second detector, used for high momentum particles, is placed after the magnet and uses $CF_4$ as the radiator. The Cherenkov light is detected with planes of photon detectors placed outside the spectrometer acceptance. Hybrid Photodiodes (HPD's) and Multi Anode phtomultipliers are being considered for the photon detectors.

### 2.5. Calorimeter system

The calorimeter system consists of a preshower detector followed by electromagnetic and hadronic calorimeters. It also serves as the initial part of the muon filter system. The cells of the Preshower detector are made up from 14 mm thick lead plates followed by square scintillators, 10 mm thick. Transverse dimensions match the segmentation of the electromagnetic calorimeter. For the electromagnetic part, a Shashlik calorimeter is used since a rather modest energy resolution is required. The hadron calorimeter is based on a scintillating tile design similar to that used in the ATLAS experiment. The required energy resolution is less severe than for ATLAS.

### 2.6. Muon system

The technology considered for the muon stations includes Multigap Resistive Plate Chambers (MRPC's) for most of the coverage and Cathode Pad Chambers (CPC's) for regions where the expected rate exceeds 5 kHz/cm$^2$. The readout pad structure is optimized for the trigger purpose.

### 2.7. Trigger

The LHCb trigger is based on four decision levels. Due to the large mass and the transverse momentum spectrum of the B-meson, its decay products have on average higher $p_{\mathrm{T}}$ than particles produced in most of the inelastic pp interactions (minimum-bias events). Decay products of the B meson originate from vertices that are displaced from the primary interaction point by several millimetres. The early levels of the LHCb trigger exploit those two characteristics. The Level-0 decision is based on high-$p_T$ hadrons or electrons found in the calorimeter system or muons found in the muon system. It provides a modest reduction of minimum-bias events by a factor of $\sim 10$. At Level-1, data from the vertex detector are used to select events with multiple vertices. Level-1 provides a reduction factor of $\sim 25$ for minimum-bias events. After a positive decision of the Level-1 trigger, data are read out to an event buffer. Hereafter, all the detector information is in principle available for the trigger decision. At Level-2, a further enhancement of events with b-hadrons is achieved by combining different detector components; for example by refining the reconstruction of the b-hadron decay vertices using momenta measured in the tracking system and information from the vertex detector. At Level-3, the trigger decision is made by reconstructing the full event. Due to the large b-hadron production rate, not all the events with b-hadrons can be recorded. Therefore, the b-hadron final states are reconstructed to select only the decay modes of interest.

Due to this trigger system, the LHCb experiment can collect a sufficient number of B-mesons with a luminosity of $\sim 2 \times 10^{32}$ cm$^{-2}$s$^{-1}$, where the number of bunch crossings with only one pp interaction is maximum. This is two orders of magnitude below the nominal LHC luminosity ensuring the physics output from the beginning of the machine operation. The luminosity is locally controlled by changing the beam focusing without affecting the other interaction regions.

## 3. CONCLUSIONS

The LHCb experiment is optimized to make a precision study of CP violation and other rare decays of B-mesons, and searches for an evidence for new physics. It is equipped with an efficient trigger and a particle identification system. The detector will be ready to exploit its physics potential from the beginning of the LHC operation expected in 2005.

## ACKNOWLEDGEMENT

The author would like to thank the organizers of the conference for their hospitality during the pleasant stay in Beijing. R. Forty is acknowledged for his various comments on this manuscript.

## REFERENCES

1. See for example reviews by
   F.J. Gilman, K. Kleinknecht and B. Renk, Eur. Phys. J. C3 (1998) 103,
   L. Wolfenstein, Eur. Phys. J. C3 (1998) 107.
2. N. Cabibbo, Phys. Rev. Lett. 10 (1963) 531,
   M. Kobayashi and K. Maskawa, Prog. Theor. Phys. 49 (1973) 652.
3. A.D. Sakharov, JETP Lett. 6 (1967) 21.
4. See for example M.B. Gavela et al., Modern Phys. Lett. 9A (1994) 795.
5. L. Wolfenstein, Phys. Rev. Lett. 51 (1983) 1945.
6. LHCb Technical Proposal, CERN LHCC 98-4 (1998).